# **Extracting Morphologic Information From Field Data**

Nathaniel G. Plant<sup>1</sup> and Rob A. Holman<sup>2</sup>

#### Abstract

We quantified the strengths and weaknesses of two sources of morphologic data available from Duck, NC, utilizing an objective definition of nearshore morphology (Gaussian curves added to a plane slope). Directly surveyed bathymetry provided the most complete estimate of the morphologic state of the nearshore bathymetry. That is, all of the parameters of the morphologic model could be estimated from these data. Oblique video images were used to estimate the position of inner bars. This information represented only a subset of the morphologic parameters defined in the morphologic model. However, the image data were collected frequently (daily) and, thus, resolved a wide range of temporal scales. Bar crest positions estimated from the video images were well correlated with estimates extracted from the bathymetric surveys ( $R^2 = 0.8$ ). Differences between the two estimates of bar position depended on both wave height and on the bar amplitude.

### 1. Introduction

Field observations of nearshore sand bar systems (Figure 1) have provided a great deal of information about the morphologic evolution (often called morphodynamics) resulting from the complicated interaction between morphology, hydrodynamics, and sediment transport (Sonu, 1973; Short, 1975, Wright and Short, 1984, and many others). Two types of measurements are commonly available to study sand bar systems. One type is visual observations, which can be made with the human eye and are a bit subjective

<sup>&</sup>lt;sup>1</sup> University of Twente, PO Box 217, WB-building, 7500 AE Enschede, The Netherlands

<sup>&</sup>lt;sup>2</sup> College of Oceanic and Atmospheric Sciences, Oregon State University, Corvallis OR 97330, USA

A. Duck, 11 Oct. 1994



Oct. 1994 B. Duck, 20 Oct. 1994



C. Noordwijk, 10 Oct. 1996



D. Agate Beach, 11 Feb. 1996



E. Palm Beach, 21 May 1997



F. Waimea, 29 Mar. 1995



Figure 1. Time exposure images of beaches from around the world, including the US East Coast (A,B), Dutch Coast (C), US West Coast (D), South Australian Coast (E), Hawaii (F). Sand bars and the shoreline may be identified by light, often shore parallel bands that correspond to shallow regions where waves tend to break.

(Short, 1975). Visual observations made with video cameras are also available (Figure 1) and these can be used more quantitatively (Lippmann and Holman, 1990). The main advantages of the video observations are that they can be made frequently (several times per day), over long time periods (decades), and they span large distances alongshore (O(km)). The primary disadvantage of visual observation methods is that, in most cases, they do not give a direct estimate of actual beach elevations.

The other technique for sampling nearshore morphology is direct bathymetric surveying. This technique gives high precision estimates of beach elevations. The primary constraint here is time, which, under the best circumstances, allows sampling of a region spanning 1 km in the cross-shore and 1 km alongshore in about 1 day (Birkemeier and Mason, 1984).

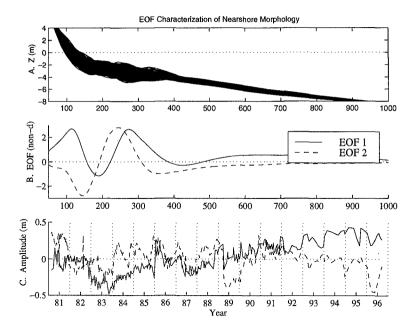


Figure 2. Analysis of beach profiles (A) using EOFs (B). The EOFs are spatial patterns describing correlated or anti-correlated beach variations. The EOFs clearly suggest the presence of sand bars. The EOF amplitudes (C) indicate the correlation of the actual profile at a particular time to each the EOF. The movement of the bars is not readily apparent from inspection of the amplitude time series.

Because of the complexity of some morphologic patterns (Figure 1d), it has been difficult to objectively define what we mean by morphology and treat the morphologic observations quantitatively. Several attempts to quantify morphology have used empirical orthogonal functions (EOFs) to represent, for example, surveyed profile data (Winant et al., 1975, and many others) and alongshore arrays of profile data (Wijnberg and Terwindt, 1995). The EOFs typically aide the analysis of morphologic variability by reducing the dimensionality of the bathymetric data (which contain observations at many spatial locations). Dimensionality is reduced by projecting observed beach elevations onto a small number of basis functions (i.e. morphologic patterns).

However, morphologic evolution described in terms of EOFs is often hard to interpret (Figure 2), since the EOFs may not have any clear physical interpretation. One example where they have been successfully interpreted is on the Dutch coast, where temporally periodic behavior was identified (Wijnberg and Terwindt, 1995). The ability to interpret the morphologic parameterization may be important when trying to constrain the morphology using two different data types. For example, video image data have been used to locate the position of surf zone sand bars (Lippmann and Holman, 1989; Lippmann and Holman, 1990; Lippmann et al., 1993). It is not clear how this information could be used to constrain any part of the morphologic patterns identified by an EOF model.

Both directly surveyed bathymetry and remotely sensed video images have different sampling strengths and weaknesses. We wish to combine the strengths of these data via an objective morphologic model. The goal of this paper is to evaluate whether the two data sources constrain a particular morphologic model in an identical manner. In section 2.1, a morphologic model for a nearshore sand bar system is defined. In section 2.2, the methods used to project the observations on the model are described. In section 3, sand bar crest position estimates (the only parameter estimated from the video data) are extracted from both surveyed bathymetry and video images. These estimates are compared and the differences analyzed. Section 4 contains both the discussion and conclusions.

### 2. Methods

## 2.1 morphologic model

We use a morphologic model that describes an alongshore-uniform, barred beach. The model consists of several Gaussian shaped sand bars superimposed upon a plane sloping beach (Figure 3). The bathymetry as a function of time (t) and cross-shore location (x) is expressed as

$$\begin{split} Z(x,t) &= \beta_1(t) + \beta_2(t) \, x + A_1(t) \exp[-\{\frac{x - X_1(t)}{L_1}\}^2] \\ &+ A_2(t) \exp[-\{\frac{x - X_2(t)}{L_2}\}^2] + A_S(t) \exp[-\{\frac{x - X_S}{L_S(t)}\}^2], \end{split} \tag{1}$$

where  $\beta_1(t) + \beta_2(t)\,x\,$  describes a plane slope component,  $A_1(t) exp[-\{\frac{x-X_1(t)}{L_1}\}^2]$ 

describes a Gaussian shaped sand bar located at  $X_1(t)$ , having a characteristic length of  $L_1$  and amplitude  $A_1(t)$ . The subscript 1 refers to an inner bar and 2 to an outer bar. The subscript "s" refers to a half-Gaussian located at the shoreline, which accommodates the shape of the subaerial beach. This model allows the true sand bars (bars 1 and 2) to change amplitude and migrate, but undergo no changes in length. The "shoreline bar" is fixed in space, but may vary its amplitude and wavelength.

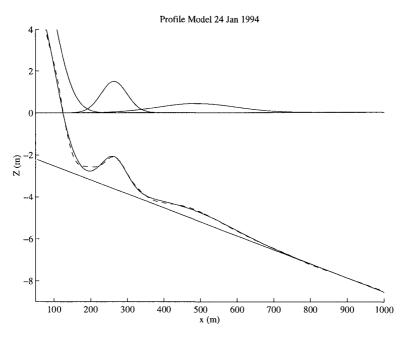


Figure 3. Example of the morphologic model (solid line), applied to FRF bathymetry (dashed line). The morphologic components of the model are shown as well.

### 2.2 Estimation of morphologic parameters

The model (1) described well the temporal and spatial variability of the bathymetric surveys obtained from the Army Corps of Engineers Field Research Facility (FRF, Figure 4). Surveys were conducted at bi-weekly and monthly intervals. The model was fit to a region north of the research pier in order to avoid inclusion of pier effects on the morphology (Figure 4). The data within a 300 m wide (alongshore) region (from . y=776 m to 1096 m) were alongshore-averaged and then fit to the morphologic model in order to extract the following 8 parameters  $\beta_1(t), \beta_2(t), A_1(t), X_1(t), A_2(t), X_2(t),$ 

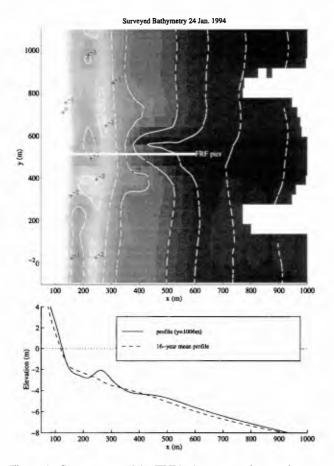


Figure 4. Contour map of the FRF bathymetry and example profile. Contour interval is 1 m.

 $A_S(t)$ ,  $L_S(t)$ .  $L_1$  and  $L_2$  were fixed at 50 m and 150 m, while  $X_s$  was fixed at 50 m. The model was fit to the alongshore averaged bathymetry using a nonlinear least squares algorithm. A typical rms error was less than 0.1 m. The rms elevation explained by the Gaussian parts of the model typically exceeded 1 m.

Since it was designed to represent bathymetric data, the model (1) could not be employed directly on video images. Instead, we assumed that the bar crest term in the model corresponded to the bar crest determined from an analysis of time exposure, video images (Lippmann and Holman, 1989 – hereafter LH89). Bar crest positions are revealed in the images by bright bands (Figure 1) that are associated foam generated in regions of wave breaking. The bar crest position data that we used are described in detail in Lippmann et al. (1993). We discuss only the estimated position of the inner bar of the commonly double-barred FRF site. We will test the correlation of the bar crest positions identified in the video images with estimates made from the bathymetric survey data.

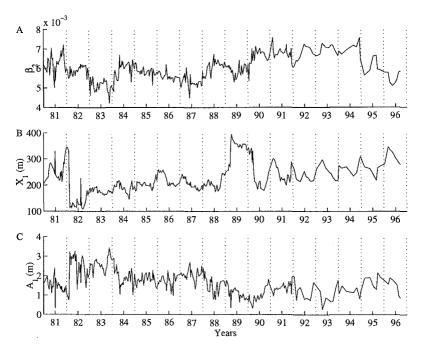


Figure 5. Time series of slope component of morphology (A), inner bar position (B), and inner bar amplitude (C). Morphologic components were extracted from the bathymetric surveys.

#### 3. Results

Figure 5 shows a time series of several morphologic parameters extracted from the FRF bathymetry. In Figure 5a, a time series of the slope parameter,  $\beta_2$ , is shown. Variation of beach slope occurred on a variety of time scales. Interestingly, there is no evidence for a long term trend. Temporal aliasing is apparent in a comparison of the time series prior to 1992 with the time series following 1992, when the sample interval changed from 0.5 months to 1 month.

Figure 5b shows a time series of the inner bar position. Rapid offshore migration occurred in Dec. 1982 and Feb. 1989. These periods correspond to offshore migration of the inner bar, followed by the generation of a new inner bar near the shoreline (apparent rapid onshore migration). These periods are marked by minimum sand bar amplitudes (Figure 5c).

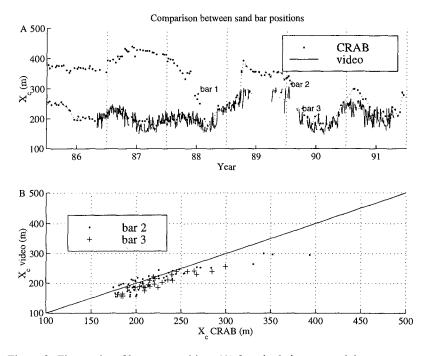


Figure 6. Time series of bar crest positions (A) from both the surveyed data sets (labeled "CRAB") and video estimates. Sand bars are labeled in order of their appearance at the FRF site. Panel B shows the correlation between survey- and video-based bar position estimates.

Figure 6 shows a time series of bar positions that were extracted from the video image time series, plotted together with time series extracted from the bathymetric data. The two time series generally correspond well with each other and clearly capture the same interannual variations of the inner bar at Duck. The image data resolve high frequency fluctuations, which may record actual variations in the bar crest position. Alternatively, the high frequency fluctuations may be related to high frequency fluctuations in the wave height, since patterns of wave breaking are used to visually identify bars in the video images.

The correlation between the time series generated from the two data sources is described in Figure 6b. The data are divided into two categories, one for bar 2 (the inner bar that formed prior to 1989, Figure 6a) and one for bar 3 (which formed after bar 2 migrated offshore to become an outer bar). The correlation, mean difference and standard deviation of the difference are shown in Table 1. The bar position identified in the video images tended to be onshore of the bar position extracted from the bathymetric surveys. This is consistent with the observations made by LH89, who attributed the shoreward bias to the persistence of foam shoreward of the bar crest. The difference in bar positions tended to increase as the bars moved farther offshore, which was not predicted by LH89.

Table 1.	Statistics	for	bar 1	position	differences
----------	------------	-----	-------	----------	-------------

rable 1. Statistics for bar position differences								
	Bar	N	$\mathbb{R}^2$	Avg. Difference	Std.			
				$(X_{video} - X_{bathy})$				
	2	60	0.78	-13 m	_21 m			
	3	27	0.85	-22 m	12 m			

Figure 7a shows a comparison of the bar position differences plotted against wave height. There was a slight tendency for the difference in bar positions to decrease as the wave height increased. The relationship is more clearly seen if the discrepancy between bar positions is plotted as a function of both wave height and bar amplitude (Figure 7b). The contours are of the mean discrepancy within 0.25 m by 0.25m ranges of wave height and bar amplitude. Only means having 95% confidence regions less than 5 m wide are shown. The mean discrepancy is smallest when both wave height and bar amplitude are high. The discrepancy increases as bar amplitude decreases and increases as wave height decreases if the bar amplitude is large. If the bar amplitude is small, the discrepancy remains large and is relatively insensitive to changes in wave height.

The difference between the two bar position estimates may simply result from the definition of a bar in terms of a deviation from the background slope, as opposed to depth minimum. In all cases, the depth minimum (if it exists) occurs where the slope of the Gaussian shaped bar is equal to, but opposite of the plane beach slope. This point is onshore of the Gaussian bar position. The fractional (relative to a bar length, L) difference between the two choices of bar position is approximately  $-(\beta_2 L)/(2 A)$ . For the Duck case, this difference was typically less than 10%, which is within the error of the estimated differences.

### 4. Discussion and Conclusions

Typically, changes in the form of nearshore bathymetry involve the evolution of a number of characteristic shapes. Ideally, it is possible to describe the bathymetry in terms of a morphologic model having only a few parameters. In addition to providing an

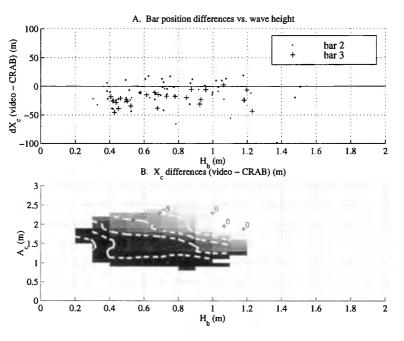


Figure 7. Analysis of discrepancy between survey and video estimates of bar crest positions. In panel A, the differences are plotted against the expected wave height at breaking (wave heights were transformed from observed wave heights using linear wave theory). Contours of the discrepancy are plotted in panel B as a function of bar amplitude and wave height.

objective definition of morphology, this step greatly reduces the dimensionality of the problem, aiding in the statistical analysis and physical interpretation of nearshore beach response.

We utilized an objective definition of nearshore morphology (Gaussian functions and a plane slope) to quantify and compare the morphologic information contained in two sources of morphologic data available from Duck, NC. Directly surveyed bathymetry provided the most complete definition of the morphologic state of the nearshore bathymetry. That is, all of the parameters of the morphologic model could be estimated from these data. Oblique video images were used to estimate the position of inner bars. This information represented only a subset of the morphologic parameters defined in the morphologic model. However, the image data were collected frequently (daily) and, thus, resolved morphologic variability over a wide range of time scales.

In a comparison, the bar positions extracted from the video images were well correlated ( $R^2 = 0.8$ ) with positions extracted from the direct surveys. Deviations between the two different estimates of bar position depended on both wave height (consistent with observations reported by LH89) and, most strongly, on the bar amplitude. An explanation for the bar amplitude dependence could be an increasing dominance of the slope morphology on the wave breaking process as bar amplitudes approached zero. LH89 point out that, even on a plane beach, a "bar" would be identified due to the presence of a maximum in wave energy dissipation. The foam generated provides the visual signal used to identify bars. The differences in the bar position estimates made from the different data sets may need to be reconciled either empirically or, perhaps, using process-based models (LH89 or Aarninkhof et al., 1998).

# 5. Acknowledgements

The video image data were graciously provided by Tom Lippmann and were published previously in Lippmann et al., 1993. The bathymetric data were provided by the Army Corps of Engineers Field Research Facility. Many different analyses of these data have been published by many other people.

#### 6. References

Aarninkhof, S. G. J., Janssen, P. C., and N. G. Plant, Quantitative estimations of bar dynamics from video images, *Proc. Coastal Dynamics '97, Plymouth*, pp.365-374, 1998.

Birkemeier, W. A. and C. Mason, The CRAB: A unique nearshore surveying vehicle, *Journal of Survey Engineering*, 110, 1-7, 1984.

Lippmann, T. C. and R. A. Holman, Quantification of sand bar morphology: A video technique based on wave dissipation, *Journal of Geophysical Research*, 94(C1), 995-1011, 1989.

Lippmann, T. C. and R. A. Holman, The spatial and temporal variability of sand bar morphology, *Journal of Geophysical Research*, 95(C7), 11,575-11,590, 1990.

Lippmann, T. C., R. A. Holman and K. K. Hathaway, Episodic, non-stationary behavior of a two sand bar system at Duck, NC, USA, *Journal of Coastal Research*, SI(15), 49-75, 1993.

Short, A. D., Three-dimensional beach stage model, *Journal of Geology*, 87, 553-571, 1975.

Sonu, C. J., Three-dimensional beach changes, Journal of Geology, 81, 42-64, 1973.

Wijnberg, K. M. and J. H. J. Terwindt, Extracting decadal morphological behavior from high-resolution, long-term bathymetric surveys along the Holland coast using eigenfunction analysis, *Marine Geology*, 126, 301-330, 1995.

Winant, C. D., D. L. Inman and C. E. Nordstrom, Description of seasonal beach changes using empirical eigenfunctions, *Journal of Geophysical Research*, 80(15), 1979-1986, 1975.

Wright, L. D. and A. D. Short, Morphodynamic variability of surf zones and beaches: A synthesis, *Marine Geology*, 56, 93-118, 1984.